

Eccentricities, fluctuations and A -dependence of elliptic and triangular flows in heavy-ion collisions

G Kh Eyyubova¹, V L Korotkikh¹, A M Snigirev^{1,2} and
E E Zabrodin^{1,3}

¹Skobeltsyn Institute of Nuclear Physics, Lomonosov Moscow State University,
RU-119991 Moscow, Russia

²Bogoliubov Laboratory of Theoretical Physics, Joint Institute of Nuclear Research,
RU-141980 Dubna, Russia

³Department of Physics, University of Oslo, PB 1048 Blindern, N-0316 Oslo, Norway

E-mail: evgeny.zabrodin@fys.uio.no

Abstract. A simple geometrical model with event-by-event fluctuations is suggested to study elliptical and triangular eccentricities in the initial state of relativistic heavy-ion collisions. This model describes rather well the ALICE and ATLAS data for Pb+Pb collisions at center-of-mass energy $\sqrt{s_{NN}} = 5.02$ TeV per nucleon pair, assuming that the second, v_2 , and third, v_3 , harmonics of the anisotropic flow are simply linearly proportional to the eccentricities ε_2 and ε_3 , respectively. We show that the eccentricity ε_3 has a pure fluctuation origin and is substantially dependent on the size of the overlap area only, while the eccentricity ε_2 is mainly related to the average collision geometry. Elliptic flow, therefore, is weakly dependent on the event-by-event fluctuations everywhere except of the very central collisions 0–2%, whereas triangular flow is mostly determined by the fluctuations. The scaling dependence of the magnitude of the flow harmonics on atomic number, $v_n \propto A^{-1/3}$, is predicted for this centrality interval.

PACS numbers: 25.75.-q, 24.10.Nz, 24.10.Pa

1. Introduction

Study of properties of new state of matter, the quark-gluon plasma (QGP), is one of the main goals of experiments on relativistic heavy-ion collisions carried out at Relativistic Heavy Ion Collider (RHIC) and Large Hadron Collider (LHC), and planned ones at coming in the nearest future Nuclotron-based Ion Collider fAcility (NICA) and Facility for Antiproton and Ion Research (FAIR); see [1, 2] and references therein. Among the signals most sensitive to the formation of QGP and its subsequent hadronization is the phenomenon known as collective flow; for reviews see, e.g., [3, 4, 5, 6]. It employs a Fourier series expansion of hadron distribution in the azimuthal plane [7, 8]

$$\frac{dN}{d\varphi} \propto 1 + 2 \sum_{n=1}^{\infty} v_n \cos [n(\varphi - \Psi_n)] . \quad (1)$$

The infinite series in the r.h.s. of Eq.(1) represent the anisotropic flow. The latter contains the flow harmonics v_n . φ is the azimuthal angle of transverse momentum of particles in the laboratory frame and Ψ_n is the symmetry plane of the n th harmonic also in the laboratory frame. The flow coefficients are calculated as

$$v_n = \langle \langle \cos [n(\varphi - \Psi_n)] \rangle \rangle , \quad (2)$$

where the averaging is taken over all hadrons in a single event and over all measured events. The first harmonics are dubbed directed, v_1 , elliptic, v_2 , triangular, v_3 , quadrangular, v_4 , flows, and so forth. Present paper deals with the study of centrality dependencies of v_2 and v_3 .

Elliptic flow has been intensively studied both theoretically [9, 10, 11, 12, 13, 14, 15, 16, 17] and experimentally [18, 19, 20, 21, 22, 23] during the last three decades. It comes from the transformation of the initial anisotropy of the overlap region in the coordinate space into the momentum anisotropy of expanding fireball. In contrast to v_2 , triangular flow in heavy-ion collisions is drawing attention in the last decade only [24, 25, 26, 27]. For a quite long period it was believed that the odd harmonics of anisotropic flow, such as v_3 , v_5 , and so on, vanishes in collisions of similar nuclei because of the symmetry considerations. However, as was first shown in [24], fluctuations in initial state (mainly, the nucleon positions) cause the triangular anisotropy ε_3 of the collision region. Triangular flow, therefore, possesses its own symmetry plane Ψ_3 , which is randomly oriented w.r.t. the position of the symmetry plane Ψ_2 of elliptic flow. Among the interesting features of both v_2 and v_3 is their approximately linear dependence on the corresponding eccentricity, ε_2 and ε_3 [28, 29, 30, 31], and their significant contribution to higher flow harmonics [32, 33, 34].

Having the LHC put into operation, one got access to a number of experimental intriguing and exquisite phenomena which would have never been systematically studied at the accelerators of previous generations. In this paper we explore and draw attention to the centrality dependence of elliptic and triangular flows. Such dependence has been thoroughly measured by the ALICE [35], ATLAS [36, 37] and CMS [38] Collaborations in $Pb+Pb$ collisions at center-of-mass energy 2.76 TeV and 5.02 TeV per nucleon pair.

In particular, these measurements demonstrate the nontrivial centrality dependence of the ratio of the second flow harmonic to the third one, which is typically missed in calculations [39] based on hydrodynamic scenario of the fireball evolution and in many phenomenological approaches; for instance, in the popular HYDJET++ model [40, 41, 42, 43]. This observation has attracted a lot of attention now; see, e.g., [44, 45, 46] and references therein. To investigate the centrality dependence of elliptic and triangular flows a simple geometrical model with event-by-event fluctuations is considered here.

The paper is organized as follows. The basic principles of the approach are described in Sec. 2. Section 3 presents the numerically calculated centrality dependencies of v_2 and v_3 in lead-lead collisions at $\sqrt{s_{NN}} = 5.02$ TeV. A fair agreement with the experimental data is obtained. In particular, we show that the profile of the overlap area, circular or elliptical, in the transverse plane is almost unimportant for the formation of triangular flow compared to the initial-state fluctuations. Dependence of both, v_2 and v_3 , in very central collisions on atomic number of colliding nuclei is discussed. Finally, conclusions are drawn in Sec. 4.

2. Formalism and modeling

The standard procedure to determine the eccentricities and the effective overlap area of two nuclei colliding with impact parameter \mathbf{b} employs Glauber eikonal model [47, 48]. For recent review describing the basic formalism see, e.g., [49]. To define the “reaction centrality” C , the cross section of particle production is subdivided into centrality bins $C_k = C_1, C_2, \dots$. The width of each bin ΔC corresponds to some fraction part of the total cross section. For instance, typical choice for most central collisions is 5% meaning that $\Delta C = 0.0 - 0.05$. Collision of two similar nuclei with radii R in this model corresponds to collision of two black disks of the same radii with centrality $C = b^2/(4R^2)$, providing us $C = 100\%$ for $b = 2R$.

Then, the thickness function $T_A(x, y)$ is the main quantity of interest in Glauber approach

$$T_A(x, y) = \int dz \rho_A(x, y, z) , \quad (3)$$

where the three-dimensional nuclear density $\rho_A(x, y, z)$ is determined via the standard Fermi-Dirac, or rather Woods-Saxon, distribution

$$\rho_A(x, y, z) = \rho_0 \frac{1}{e^{(r-R)/d} + 1} . \quad (4)$$

Here R is the nuclear radius, A is its atomic number, d is the diffuseness edge parameter and ρ_0 is a normalization constant, so that $\int \rho_A(r) d^3r = A$.

The needed eccentricities are calculated by the standard formulas

$$\begin{aligned} \varepsilon_n &= \varepsilon_{n,x} + i\varepsilon_{n,y} = \frac{\int s ds d\phi e^{in\phi} s^n w(\mathbf{s}, \mathbf{b})}{\int s ds d\phi s^n w(\mathbf{s}, \mathbf{b})} , \\ |\varepsilon_n|^2 &= \varepsilon_{n,x}^2 + \varepsilon_{n,y}^2 , \end{aligned} \quad (5)$$

where $w(\mathbf{s}, \mathbf{b})$ are some weights, $s^2 = x^2 + y^2$, and $\tan \phi = y/x$. Under the assumption of some “macroscopic” overlap between the colliding nuclei one can define the transverse overlap area as [50]

$$S(b) = 4\pi\sqrt{\langle x^2 \rangle \langle y^2 \rangle}, \quad (6)$$

where the weighted averages are the same as in Eq.(5). Recall that one lacks unique definition of the absolute normalization of the overlap area. In our definition the overlap area has maximum magnitude 4π , which is four times larger than, e.g., that defined in Ref. [7]. On the other hand, it almost coincides with the geometrical overlap area between two disks possessing uniform two-dimensional density distribution.

The next step is a choice of weights, which is ambiguous and is determined in the specific models. Often the number of binary nucleon-nucleon collisions in an $A + B$ collision at given impact parameter \mathbf{b} is used as weights. In this case up to the inessential normalization factor they are equal to

$$w(\mathbf{s}, \mathbf{b}) = T_A(x + b/2, y)T_B(x - b/2, y) \quad (7)$$

with the impact parameter \mathbf{b} being directed along the x -axis. Other weights are possible too, for instance, the number of participating nucleons. This problem was partly discussed in [50] with calculations of second eccentricity ε_2 for various nucleon densities as a function of b . In particular, at a small value of diffuseness edge parameter d the eccentricity ε_2 is close to the pure geometrical one

$$\varepsilon_{2,\text{geom}} = b/(2R) = \sqrt{C}. \quad (8)$$

In this approach the third eccentricity ε_3 , as well as the other odd ones, is identically equal to zero if the three-dimension nuclear density $\rho_A(x, y, z)$ depends on the radial distance r only (a spherically symmetric distribution of matter in the Breit system).

Here one should note that nuclei consist of a finite number of nucleons which have the finite sizes and their positions are distributed in accordance with Eq.(4). The nucleon positions can fluctuate in event-by-event. These fluctuations were taken into account in Monte Carlo Glauber calculations [48] and subsequently with the realization that odd flow coefficients would be non-zero [24]. The energy deposition in the overlap region of two nuclei can also be used as weights taking into account its fluctuations [44, 45]. Both approaches are discussed and reviewed in the subsections below.

2.1. Geometrical model with fluctuations

In the simplest model of hard spheres the nuclei have a spherical shape of radius R with uniformly distributed nucleon density

$$\rho_A(x, y, z) = \frac{3}{4\pi R^3} \Theta(r - R). \quad (9)$$

In this case the eccentricities and the effective overlap area in the non-central collision of two nuclei with the impact parameter \mathbf{b} are calculated in an analytic form that are often used as a first good approximation.

The model can be improved by taking into account the fluctuations of nucleon positions. Note that the integration in Eq.(5) can be performed by the Monte Carlo method. The accuracy of estimation is limited by the number of points in which weights are calculated. Therefore, we opted to calculate the integrals in Eq.(5) by the Monte Carlo method with the *finite fixed number* of points M over each of coordinate, x and y . In this approach a single event represents the location of M^2 points in the x - y plane. At this simple modeling the number M^2 is a some analogue of the number of the participant nucleons or colour charges used in other models. Then, one should average over ensemble of such events with the fixed finite number of points. As a result of averaging procedure $\langle \varepsilon_{3,x} \rangle = \langle \varepsilon_{3,y} \rangle = 0$, but

$$\varepsilon_3\{2\} = \sqrt{\langle |\varepsilon_3|^2 \rangle} \quad (10)$$

will be non-zero as well as

$$\varepsilon_2\{2\} = \sqrt{\langle |\varepsilon_2|^2 \rangle} \quad (11)$$

at $C = 0$ in contrast to “continuous” ($M \rightarrow \infty$) calculations (8). The number of points, in which weights are calculated at $C = 0$, is a single parameter which should be fitted to reproduce data.

2.2. Magma model

The resulting profile of energy density in an ultrarelativistic nucleus-nucleus collision is simulated as the sum of contributions of elementary collisions between a localized color charge and a dense nucleus. Each elementary collision yields a source of energy density which is independent of rapidity and decreases with distance from the center of the source. Thus, the energy density $\rho(\mathbf{r}, \mathbf{b})$ as a function of the transverse distance \mathbf{r} and the impact parameter \mathbf{b} is determined by the product of the saturation momentum squared Q^2 of one nucleus (where $1/Q^2$ is related to an effective “area” of each colour charge in the transverse region) and the random source depositions of other nucleus [44]

‡

$$\begin{aligned} \rho(\mathbf{r}, \mathbf{b}) = & \sum_{j \subset A} Q_B^2(\mathbf{s}_{A,j}, \mathbf{b}) \Delta_A(\mathbf{r} - \mathbf{s}_{A,j}, \mathbf{b}) \\ & + \sum_{j \subset B} Q_A^2(\mathbf{s}_{B,j}, \mathbf{b}) \Delta_B(\mathbf{r} - \mathbf{s}_{B,j}, \mathbf{b}) . \end{aligned} \quad (12)$$

Here Q_A and Q_B are the saturation momenta of the colliding nuclei A and B to be specified below. The positions $\mathbf{s}_{A,j}$ and $\mathbf{s}_{B,j}$ are assumed to be independent random variables.

The profile Δ of energy source in nucleus (A/B) is selected in the form which satisfies the short distance correlations in the Color Glass Condensate (CGC) approach

‡ We are aware that the Magma authors pointed out a potential problem with the CGC correlator employed in the model. This correlator is not directly used in our study.

[51, 52, 53]

$$\Delta(\mathbf{r} - \mathbf{s}_{A,j}, \mathbf{b}) = \left\{ \begin{array}{ll} \frac{8}{g^2 N_c} \frac{1}{|\mathbf{r} - \mathbf{s}_{A,j}|^2 + Q_A^{-2}(\mathbf{r}, \mathbf{b})}, & |\mathbf{r} - \mathbf{s}_{A,j}| < 1/m \\ 0, & |\mathbf{r} - \mathbf{s}_{A,j}| > 1/m \end{array} \right\}, \quad (13)$$

where g is the dimensionless coupling constant of QCD, N_c is the number of colors ($N_c = 3$ for QCD), and m is the infrared cutoff parameter of the order of pion mass. At large distance $\Delta(\mathbf{r})$ decreases like $1/r^2$ as for a Coulomb field in two dimensions. However, $\Delta(\mathbf{r})$ goes to a finite value for $r \rightarrow 0$, while it would diverge for a pointlike charge. The physical interpretation is that the charge is spread over a distance $\sim 1/Q_A$. The number of elementary charges contained in an area of this size is of the order $1/g^2$, which explains the normalization factor arising in Eq.(13).

If a source is located in the region of the nuclear size, then the distribution (13) is concentrated inside an area with radius $|\mathbf{r}| < 1/m = 1.4$ fm. It is considerably smaller than the transverse area of heavy nuclei (for instance, for lead nucleus with radius $R = 6.62$ fm). At $\mathbf{s}_{A,j} = \mathbf{r}$ the energy intensity reaches maximum in the nuclear center and is proportional to $Q_A^2(\mathbf{r}, \mathbf{b})$. The integral intensity of one source, to the leading logarithm accuracy, reads

$$I_A(\mathbf{r}, \mathbf{b}) = \int d^2s \Delta(\mathbf{r} - \mathbf{s}, \mathbf{b}) \simeq \frac{8\pi}{g^2 N_c} \ln \left[1 + \frac{Q_A^2(\mathbf{r}, \mathbf{b})}{m^2} \right]. \quad (14)$$

In the Magma model Q_A^2 is assumed to be proportional to the integral of the nuclear density over the longitudinal coordinate z , i.e., to the thickness function

$$Q_A^2(x, y) = Q_{s0}^2 T_A(x, y) / T_A(0, 0). \quad (15)$$

The value of the saturation momentum Q_{s0} at the nucleus center is a free parameter in this approach and the energy density $\rho(\mathbf{r}, \mathbf{b})$ is applied as weights in calculations of eccentricities (5).

The number of sources per unit area (density) is eventually given by

$$n_A = \frac{N_c^2}{32\pi} \frac{Q_A^2(\mathbf{r}, \mathbf{b})}{\ln \left[1 + \frac{Q_A^2(\mathbf{r}, \mathbf{b})}{m^2} \right]}. \quad (16)$$

Thus, the maximum number of sources in the nuclear transverse area with radius $R = 6.62$ fm at $Q_{s0} = 1.24$ GeV is approximately calculated as $N_{\text{Pb}} \simeq 100$. Note, that the parameter $1/\sqrt{N_{\text{Pb}}}$ can characterize the fluctuation scale.

2.3. (Improved) Monte Carlo Glauber model

The Monte Carlo (MC) Glauber model [47, 48, 49] is widely used in analysis of experiments with relativistic heavy-ion collisions. It relates the initial collision geometry to the measured observables. Its basic principles have been already discussed in the beginning of this Section. Recall, that the MC Glauber model treats nucleus-nucleus collisions as a superposition of independent nucleon-nucleon collisions. The positions of nucleons relative to the geometrical centers of colliding nuclei are assumed to be

randomly distributed in space according to Woods-Saxon spherical density $\rho(\vec{r})$, see Eq.(4). Quite often, this distribution is taken from the available experimental data. Nucleons interact if the distance between their centers is less than $\sqrt{\sigma_{inel}^{NN}/\pi}$, where σ_{inel}^{NN} is the inelastic cross section of NN interaction. In eikonal approximation nucleons move along straight-line trajectories. To improve the modeling, it was also suggested to employ NN correlations [54].

In the present paper we use the improved MC Glauber model described in [55]. In contrast to standard MC Glauber model, the improved model implements separated transverse profiles for neutrons and protons in heavy nuclei, such as gold or lead ones. The positions of nucleons inside a nucleus are modeled to provide a minimum separation in order to emulate hard-core repulsion between nucleons. The latter should not, however, distort the nuclear density.

It is worth mentioning that in MC Glauber model the number of participants serves as weights for eccentricity calculations. Therefore, all three models at our disposal rely on different weighting schemes: MC hard sphere model uses the number of binary collisions, Magma model employs the energy density, and MC Glauber model applies the number of participants. In the next Section we will see how these differences affect the estimations of elliptic and triangular eccentricities and related to it elliptic and triangular flows in heavy-ion collisions.

3. Results

The formalism briefly reviewed in Sec. 2 is applied to calculate the initial eccentricities ε_2 and ε_3 as functions of the geometrical centrality C in relativistic heavy-ion collisions. Values accessible experimentally are moments or cumulants of the distribution of the flow harmonic coefficients v_n . The lowest order cumulants are defined as [56]

$$v_n\{2\} = \sqrt{\langle |v_n|^2 \rangle}. \quad (17)$$

In the linear response approximation they are simply proportional to the corresponding cumulants of the initial eccentricities [32]

$$\begin{aligned} v_2\{2\} &= k_2 \varepsilon_2\{2\}, \\ v_3\{2\} &= k_3 \varepsilon_3\{2\}. \end{aligned} \quad (18)$$

Typically, the cumulants are measured over the two-particle correlations defined as

$$\langle\langle 2 \rangle\rangle = \langle\langle e^{in(\varphi_1 - \varphi_2)} \rangle\rangle = (v_n\{2\})^2. \quad (19)$$

Here the double averaging $\langle\langle \rangle\rangle$ is performed over all particle combinations and over all events; see, e.g., [43] for the definition of the differential and other cumulants over particle correlations. For the collisions with centrality from 0% to 30% the Magma model describes successfully [44] the experimental data on v_2 and v_3 as functions of centrality percentile, measured by the ATLAS Collaboration [37] in $Pb+Pb$ collisions at $\sqrt{s_{NN}} = 5.02$ TeV. The proportionality coefficients $k_2 = 0.321$ and $k_3 = 0.314$ together with the saturation momentum $Q_{s0} = 1.24$ GeV were adjusted to data. This set of

parameters was employed to calculate the centrality dependence of the eccentricities ε_2 and ε_3 . Obtained results are compared with predictions of other models, such as Monte Carlo hard sphere, hard sphere, and Monte Carlo Glauber model, in Fig. 1. Recall that for calculations we used the improved Monte Carlo Glauber model, described in [55]. Cross section $\sigma_{NN} = 67.6$ mb was picked up from Table III of this paper.

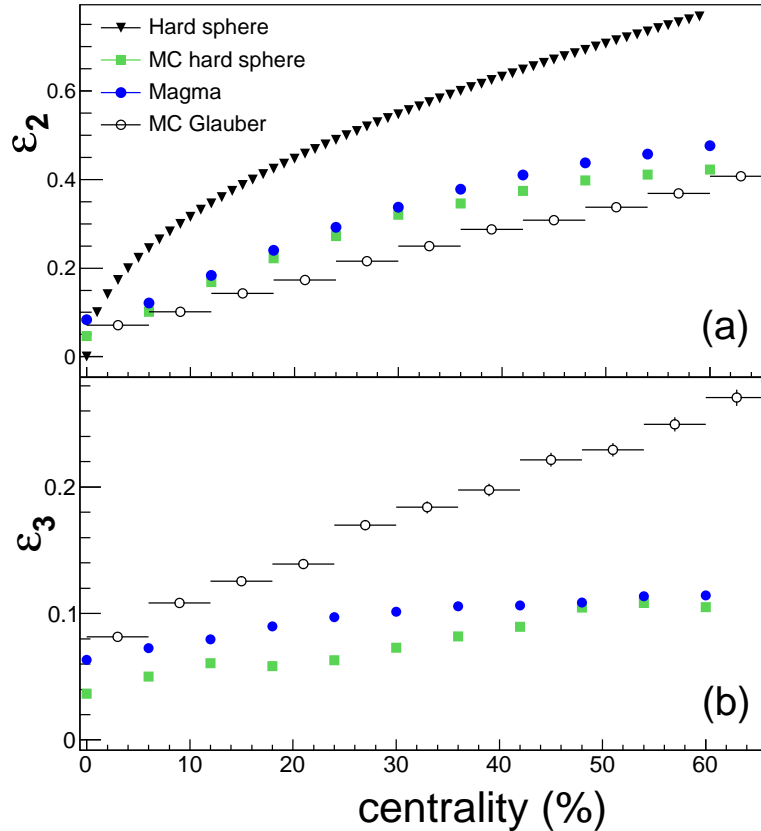


Figure 1. (Color online) The eccentricities (a) ε_2 and (b) ε_3 as functions of centrality C for hard sphere model (triangles), Monte Carlo hard sphere model (squares), Magma model (full circles), and Monte Carlo Glauber model (open circles).

In Fig. 1(a) one can see that the elliptic eccentricity ε_2 calculated in the Magma model is very close to that obtained in the Monte Carlo hard sphere model within the centrality interval 2–30%. Note, that for the very central collisions with $\sigma/\sigma_{geo} = 0-2\%$ both Magma and MC hard sphere eccentricities go to a finite value, whereas the geometrical $\varepsilon_2 = b/(2R)$ goes to zero at $C \rightarrow 0$. Calculations of MC Glauber model are qualitatively similar to those of two other MC models (MC Hard sphere, Magma) but lie about 20 – 30% below. For the triangular eccentricity, shown in Fig. 1(b), the Magma model overpredicts the MC hard sphere results by 25–40% for centralities $C \leq 40\%$. For more peripheral collisions predictions of both models quickly converge. The MC Glauber model significantly overpredicts the calculations of both, MC hard sphere and

Magma, models. Recall, that the odd-order eccentricities are zero in the hard sphere (HS) model, therefore, ε_3^{HS} is absent in this figure.

In contrast to the second eccentricity coefficient determined by the shape of the overlap region and, therefore, mainly by the collision geometry, the third eccentricity coefficient is of a pure fluctuation origin. Its magnitude is practically determined by the overlap region area, but not its shape. The indirect evidence of this affirmation follows from the fact that the ratio $\sqrt{\langle v_3^2 \rangle - \langle v_3 \rangle^2} / \langle v_3 \rangle$ is nearly constant at all centralities and is slightly dependent on the transverse momentum. The sensitivity to the overlap shape can be tested by the variation of the diffuseness edge parameter d . We found that, unlike the second eccentricity ε_2 which is noticeably dependent of d , the third eccentricity is practically insensitive to the diffuseness variation, i.e., to the shape of overlap region. Figure 2 illustrates these statements. Indeed, in the simple model of hard sphere one can easily calculate the area of the overlap region $S(C) \simeq \pi R^2(1 - \sqrt{C})$ and, therefore, the number of “source-points” $N_{\text{points}} = \text{density} \times S(C)$. If the third harmonic has a pure fluctuation origin then its magnitude reads

$$v_3(C) \sim \frac{1}{\sqrt{N_{\text{points}}}} \simeq \frac{K_3}{\sqrt{1 - C^{1/2}}} . \quad (20)$$

This pure fluctuation centrality dependence (20) is shown in Fig. 2(a),(b) in comparison with experimental data. With $K_3 = 0.0183$ we obtain a good description of the data in the centrality region below 50%.

To demonstrate that the area of the overlap region has the significance only, while the shape is unimportant, we display in Fig. 2(c),(d) the triangular flow v_3 calculated for perfectly central collisions with $b = 0$, but with the radius changing as

$$R(C) = R\sqrt{1 - C^{1/2}} . \quad (21)$$

In this case the overlap region has circular shape, see Fig. 2(d). However, the area of the circle is the same as the overlap area in the hard sphere model at given centrality C . As one can see in Fig. 2(c), a good agreement with the experimental data is obtained despite of the fact that no new parameters were either introduced or tuned in the model.

Figure 3 shows the elliptic $v_2\{2\}$ and triangular $v_3\{2\}$ flows, calculated by two-cumulant method [56] as functions of centrality C in the linear response approximation, given by Eq.(18), with the *constant* coefficients adjusted to data. We see that for more peripheral collisions with centralities larger than 30% a linear dependence $v_2(C) = k_2\varepsilon_2(C)$ with constant coefficients k_2 is not realized, since the second eccentricity $\varepsilon_2\{2\}$ becomes too large. The k_2 “hydro” conversion coefficient is expected to change with centrality, smaller in peripheral collisions, and nonlinear effects come into play.

The results of MC Glauber model for $v_2(C)$, presented in Fig. 3(a), demonstrate weaker elliptic flow compared to that of two other MC models in the centrality range $5\% \leq C \leq 50\%$. The flow measured by the ALICE Collaboration lies between the three model calculations. It implies that elliptic flow is mainly determined by the geometry of the overlap region, whereas fluctuations play a minor role for all but very central collisions. For the triangular flow, displayed in Fig. 3(b), the fluctuations induced by

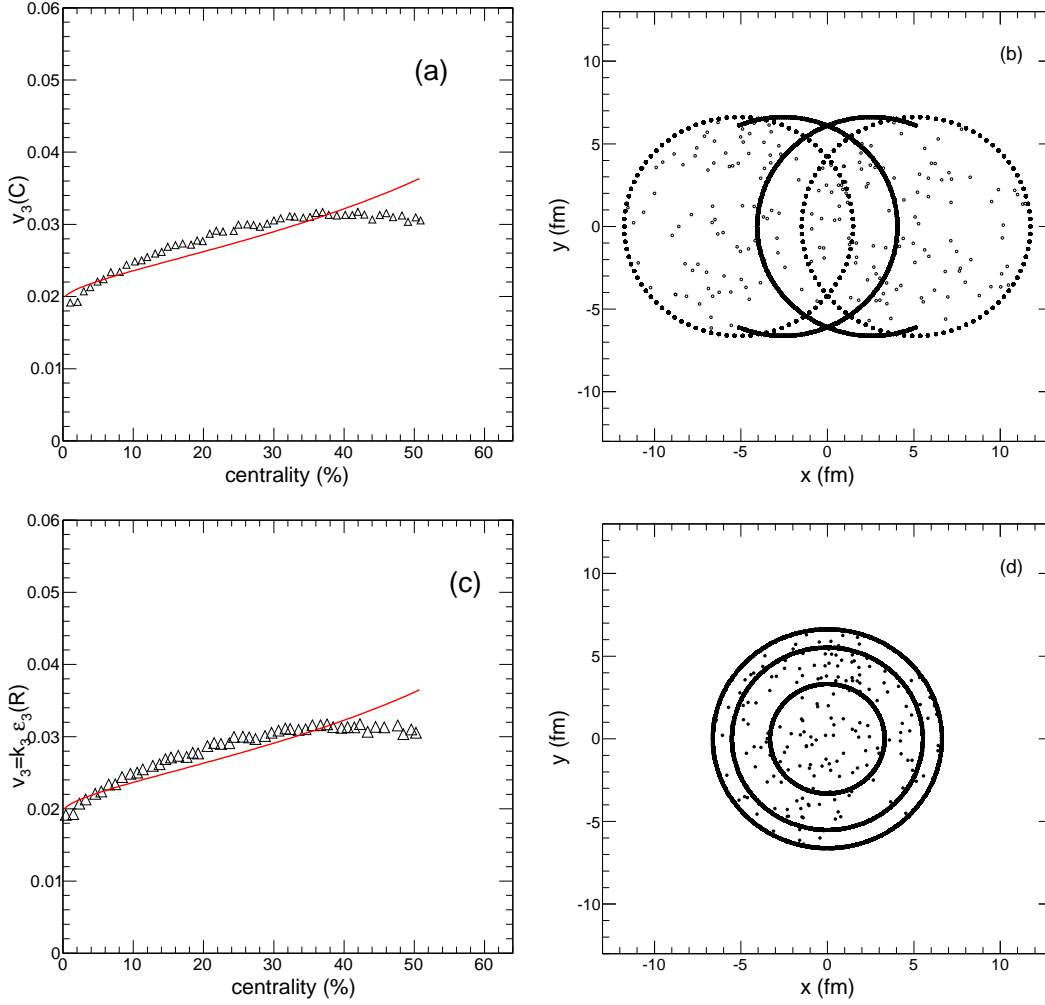


Figure 2. (Color online) (a) Centrality dependence of triangular flow in $Pb+Pb$ collisions at $\sqrt{s_{NN}} = 5.02$ GeV. Solid line shows the calculations in accordance with Eq. (20), whereas open triangles denote the ALICE data from [35] in $Pb+Pb$ collisions at center-of-mass energy 5.02 TeV per nucleon pair within the transverse momentum interval $0.2 < p_T < 50$ GeV/c and within the pseudorapidity interval $|\eta| < 0.8$. A separation in pseudorapidity between the correlated particles $|\Delta\eta| > 1$ is applied. All observables are calculated in small centrality bins (1%). (b) Changing of the overlap region in transverse plane with variation of the collision centrality from $C = 12\%$ (solid curves) to 60% (dashed curves). Dots show the positions of the sources. See text for details. (c) Triangular flow calculated in both models (solid curve) at $b = 0$ with the radius variation in accordance with Eq. (21) and at $k_3 = 0.314$ in Eq. (18). The radius of the circle is varying to provide the same area as that of the overlap region of $Pb+Pb$ collisions at certain centrality. Open triangles denote the ALICE data from [35]. (d) Changing of the overlap area with the radius variation from $R = 6.62$ fm (outer circle) to 5.3 fm (inner circle) and 3.1 fm (most inner circle). Dots show the positions of the sources. See text for details.

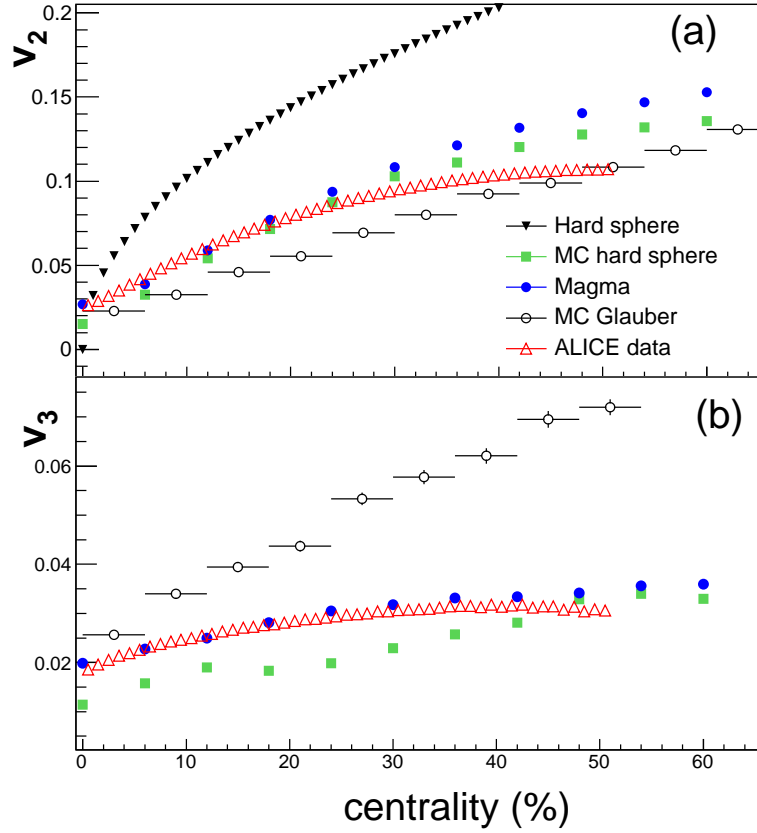


Figure 3. (Color online) The elliptic $v_2\{2\}$ and triangular $v_3\{2\}$ flows as functions of centrality C for hard sphere model (full triangles), Monte Carlo hard sphere models (full squares), Magma model (full circles), and MC Glauber model (open circles). Open triangles denote the ALICE data from [35] measured in $Pb + Pb$ collisions at center-of-mass energy 5.02 TeV per nucleon pair within the transverse momentum interval $0.2 < p_T < 50$ GeV/ c and within the pseudorapidity interval $|\eta| < 0.8$. A separation in pseudorapidity between the correlated particles $|\Delta\eta| > 1$ is applied. All observables are calculated in small centrality bins (1%).

the MC Glauber model are too strong compared to data, leaving room for further tuning of model parameters.

The “pure fluctuation” contribution to the second harmonic reveals itself in the most central collisions with $\sigma/\sigma_{geo} = 0 - 2\%$ only, where the “pure geometrical” contribution goes to zero. This explains also the interesting observation that the ratio $v_2/v_3 = 1$ at $C = 0$. One should note that the absolute magnitude of both harmonics within this centrality interval is merely determined by the number of sources, i.e., by the area of overlap region. It means that MC models predict the larger values of elliptic and triangular flows in very central collisions for the lighter nuclei, because v_2 and v_3

turn out to scale with the atomic number to the $1/3$ power

$$v_n^{AA}(C=0) = v_n^{PbPb}(C=0) \left(\frac{208}{A} \right)^{1/3}. \quad (22)$$

Indeed, the number of “source-points” is proportional to the area of the overlap region, i.e. R^2 , and in accordance with “the fluctuation scenario” given by Eq.(20) we get

$$v_3(C) \sim \frac{1}{\sqrt{N_{\text{sources}}}} \sim \frac{1}{\sqrt{R^2}} \sim \frac{1}{R} \sim A^{-1/3}. \quad (23)$$

For lighter colliding system, such as $Xe+Xe$, both v_2 and v_3 will increase by factor of 1.17 compared to $Pb+Pb$ central collisions, whereas for $Cu+Cu$ Eq.(22) predicts 1.5 stronger flows. ALICE Collaboration in [57] presented the measurements of the flow harmonics of charged particles in $Xe+Xe$ collisions at $\sqrt{s_{NN}} = 5.44$ TeV. Both v_2 and v_3 , measured in the $Xe+Xe$ collisions at centralities from 3% to 7%, are larger than those in $Pb+Pb$ collisions measured at $\sqrt{s_{NN}} = 5.02$ TeV; see Fig. 2 of [57]. This is qualitatively in line with our predictions. However, only result for triangular flow is in a perfect agreement with our estimate of the increase by 1.17. Elliptic flow in $Xe+Xe$ collisions at the same centralities appears to be 1.35 times stronger than that in $Pb+Pb$ collisions, indicating the influence of the collision geometry. Also, the elliptic flow in $Cu+Cu$ collisions at RHIC energies was measured by the STAR Collaboration in [58]. Unfortunately, no results for triangular flow were presented, and the most central bin was 0-10%. Here the role of pure fluctuations in the v_2 is significantly obscured. It would be interesting to check this $A^{-1/3}$ dependence for other colliding systems as well.

4. Conclusion

The role of (i) shape of the overlap area of noncentral nuclear collisions and (ii) fluctuations of interacting centers, called *sources*, in the formation of elliptic and triangular flows are studied within the MC hard sphere, MC Glauber, and Magma models. Our investigation shows that the third flow harmonic v_3 has merely fluctuation origin. Its centrality dependence is determined by the variation of the overlap area with the changing centrality of heavy-ion collisions C and is well fitted to the simple “fluctuation” formula given by Eq.(20). In contrast, elliptic flow coefficient v_2 is closely related to the collision geometry. The “fluctuation” contribution to v_2 reveals itself in the most central collisions $\sigma/\sigma_{geo} = 0 - 2\%$ only. In this centrality interval the absolute value of all harmonics is simply determined by the number of “source-points” and is independent of the shape of the overlapping region. Both MC hard sphere and Magma models give quite interesting prediction for the behavior of magnitude of all harmonics with the variation of atomic number A . Namely, the magnitude of the signal should scale as $A^{-1/3}$ in the most central collisions (0 – 2%). This prediction is in a very good agreement with the experimental results obtained by ALICE Collaboration for measurements of v_3 in $Xe+Xe$ collisions at $\sqrt{s_{NN}} = 5.44$ TeV and $Pb+Pb$ collisions at $\sqrt{s_{NN}} = 5.02$ TeV [57], but underestimates the effect for v_2 which appears to be 1.35 times stronger in semi-central $Xe+Xe$ collisions. To get rid of additional effects caused

by collision geometry, here one has to go to very central collisions. Recall, that this centrality region is under intensive theoretical and experimental study now; see, e.g., recent paper [46] and references therein. The calculated initial eccentricities ε_2 and ε_3 can be used as an input to phenomenological models like the HYDJET++ to improve the description of the centrality dependence of the flow azimuthal characteristics.

Acknowledgments

Fruitful discussions with A.I. Demyanov, C. Loizides and I.P. Lokhtin are gratefully acknowledged. This work was supported in parts by Russian Foundation for Basic Research (RFBR) under Grants No. 18-02-40084 and No. 18-02-40085, and by Norwegian Agency for International Cooperation (SIU) under Grant UTF-2016-long-term/10076. E.E.Z. acknowledges support of the Norwegian Research Council (NFR) under grant No. 255253/F50, “CERN Heavy Ion Theory.”

References

- [1] Liu F, Wang E, Wang X-N, Xu N and Zhang B-W (eds) 2021 *Proc. of Quark Matter 2019 Nucl. Phys. A* **1005** 122104
- [2] Antinori F, Dainese A, Giubellino P, Greco V, Lombardi M P and Scapparini E (eds) 2019 *Proc. of Quark Matter 2018 Nucl. Phys. A* **982** 1-1066
- [3] Reisdorf W and Ritter H G 1997 *Ann. Rev. Nucl. Sci.* **47** 663
- [4] Herrmann N, Wessels J P and T. Wienold T 1999 *Ann. Rev. Nucl. Sci.* **49** 581
- [5] Voloshin S A, Poskanzer A M and Snellings R 2010 *Relativistic Heavy Ion Physics (Landolt-Boernstein vol 23)* ed R Stock (Springer, Berlin) p 293
- [6] Heinz U and Snellings R 2013 *Annu. Rev. Nucl. Part. Sci.* **64** 123
- [7] Voloshin S and Zhang Y 1996 *Z. Phys. C* **70** 665
- [8] Poskanzer A M and Voloshin S A 1998 *Phys. Rev. C* **58** 1671
- [9] Ollitrault J-Y 1992 *Phys. Rev. D* **46** 229
- [10] Ollitrault J-Y 1993 *Phys. Rev. D* **48** 1132
- [11] Sorge H 1999 *Phys. Rev. Lett.* **82** 2048
- [12] Zabrodin E E, Fuchs C, Bravina L V and Faessler Amand 2001 *Phys. Lett. B* **508** 184
- [13] Teaney D 2003 *Phys. Rev. C* **68** 034913
- [14] Molnar D and Voloshin S A 2003 *Phys. Rev. Lett.* **91** 092301
- [15] Schenke B, Jeon S and Gale C 2011 *Phys. Rev. Lett.* **106** 042301
- [16] Ruggieri M, Scardina F, Plumari S and Greco V 2013 *Phys. Lett. B* **727** 177
- [17] Le Fevre A, Leifels Y, Hartnack C and Aichelin J 2018 *Phys. Rev. C* **98** 034901
- [18] Ackermann K H et al (STAR Collaboration) 2001 *Phys. Rev. Lett.* **86** 402
- [19] Adler S S et al (PHENIX Collaboration) 2003 *Phys. Rev. Lett.* **91** 182301
- [20] Aamodt K et al (ALICE Collaboration) 2010 *Phys. Rev. Lett.* **105** 252302
- [21] Aad G et al (ATLAS Collaboration) 2012 *Phys. Lett. B* **707** 330
- [22] Chatrchyan S et al (CMS Collaboration) 2012 *Eur. Phys. J. C* **72** 2012
- [23] Adamczyk L et al (STAR Collaboration) 2013 *Phys. Rev. C* **88** 014902
- [24] Alver B and Roland G 2010 *Phys. Rev. C* **81** 054905
- [25] Alver B H, Gomeaud C, Luzum M and Ollitrault J-Y 2010 *Phys. Rev. C* **82** 034913
- [26] Aamodt K et al (ALICE Collaboration) 2011 *Phys. Rev. Lett.* **107** 032301
- [27] Schenke B, Jeon S and Gale C 2012 *Phys. Rev. C* **85** 024901
- [28] Velkovska J et al (CMS Collaboration) 2011 *J. Phys. G: Nucl. Part. Phys.* **38** 124011

- [29] Jia J et al (ATLAS Collaboration) 2011 *J. Phys. G: Nucl. Part. Phys.* **38** 124012
- [30] Snellings R et al (ALICE Collaboration) 2011 *J. Phys. G: Nucl. Part. Phys.* **38** 124013
- [31] Petersen H, Qin G-Y, Bass S A and Müller B 2010 *Phys. Rev. C* **82** 041901
- [32] Gardim F G, Grassi F, Luzum M and Ollitrault J-Y 2012 *Phys. Rev. C* **85** 024908
- [33] Teaney D and Yan L 2012 *Phys. Rev. C* **86** 044908
- [34] Bravina L V, Brusheim Johansson B H, Eyyubova G Kh et al 2014 *Phys. Rev. C* **89** 024909
- [35] Acharya S et al (ALICE Collaboration) 2018 *J. High Energy Phys.* **07** 103
- [36] Aad G et al (ATLAS Collaboration) 2012 *Phys. Rev. C* **86** 014907
- [37] Aaboud M et al (ATLAS Collaboration) 2020 *J. High Energy Phys.* **01** 51
- [38] Chatrchyan S et al (CMS Collaboration) 2014 *Phys. Rev. C* **89** 044906
- [39] Alba P, Mantovani V, Noronha J et al 2018 *Phys. Rev. C* **98** 034909
- [40] Lokhtin I P, Malinina L V, Petrushanko S V et al 2009 *Comput. Phys. Commun.* **180** 779
- [41] Bravina L V, Brusheim Johansson B H, Eyyubova G Kh et al 2014 *Eur. Phys. J. C* **74** 2807
- [42] Eyyubova G, Bravina L V, Korotkikh V L et al 2009 *Phys. Rev. C* **80** 064907
- [43] Bravina L V, Eyyubova G Kh, Korotkikh V L et al 2021 *Phys. Rev. C* **103** 034905
- [44] Gelis F, Giacalone G, Guerrero-Rodriguez P et al 2019 *Primordial fluctuations in heavy-ion collisions* arXiv:1907.10948 [nucl-th]
- [45] Floerchinger S, Grossi E and Yousefnia K V 2020 *Phys. Rev. C* **102** 054914
- [46] Zakharov B G 2020 *JETP Lett.* **112** 393
- [47] Glauber R J 1959 *Lectures in Theoretical Physics* vol 1 eds W E Brittin and L G Dunham (Interscience, New York) p 315
- [48] Miller M L, Reygers K, Sanders S J and Steinberg P 2007 *Annu. Rev. Nucl. Part. Sci.* **57** 205
- [49] d’Enterria D and Loizides C 2020 *Progress in the Glauber model at collider energies* arXiv:2011.14909 [hep-ph]
- [50] d’Enterria D, Eyyubova G Kh, Korotkikh V L et al 2010 *Eur. Phys. J. C* **66** 173
- [51] Krasnitz A and Venugopalan R 2000 *Phys. Rev. Lett.* **84** 4309
- [52] Lappi T 2006 *Phys. Lett. B* **643** 11
- [53] Albacete J L, Guerrero-Rodriguez P and Marquet C 2019 *J. High Energy Phys.* **01** 073
- [54] Alvioli M, Dresher H-J and Strikman M 2009 *Phys. Lett. B* **680** 225
- [55] Loizides C, Kamin J and d’Enterria D 2018 *Phys. Rev. C* **97** 054910
2019 Erratum: *Phys. Rev. C* **99** 019901
- [56] Borghini N, Dinh P M and Ollitrault J-Y 2001 *Phys. Rev. C* **64** 054901
- [57] Acharya S et al (ALICE Collaboration) 2018 *Phys. Lett. B* **784** 82
- [58] Abelev B I et al (STAR Collaboration) 2010 *Phys. Rev. C* **81** 044902